Computer aided Engineering of Filter Materials and pleated Filters

A. Wiegmann, O. Iliev, A. Schindelin

New legislation, new materials, globalization and short development cycles require deeper understanding of filter materials and particle filtration processes than ever before. Detailed computer simulations are a recent, efficient way to gain valuable insights into these topics. The scales where filtration phenomena can be observed range from the macroscopic regime of flow around a moving vehicle to the atomic regime of adhesion forces between dust particles and an electrically charged filter medium. These scale differences necessitate a complex modeling approach. Fortunately, powerful computers, detailed models and new experimental equipment are available. Desktop computers with large memory and multi-core architecture as well as three-dimensional models combined with Scanning Electron Microscope (SEM) and micro Computer Tomography (μCT) images are some of the exciting developments that allow work today that was unthinkable even in the recent past. We give a general idea how this works and a concrete example how simulations have helped to design and patent a new filter element.

Keywords
Filtration, Simulation, Filter Media, Pleated Filter, Pressure Drop.

1. Introduction

Particle Filtration is a highly complex phenomenon that poses countless challenges to modeling and simulation, most notably through the large differences in scales that come into play. Figure 1 illustrates the scales and applications where these scale considerations might stem from.

A fluid (gas or liquid) transports the particles to the filter and through the filter media. Due to the difference in scales, the simulation of this flow must be considered as two separate tasks. In the free flow up to the filter media, the main concerns are the lowest possible pressure drop, equal distribution of particles to the filter, and the handling of the physical properties of the flow, for example turbulence. Within the filter media, the challenges lie in the facts that the precise geometry of the filter media is usually not known, and in imposing the influence of this geometry on the flow field. When particles are added to this system, they interact with the fluid and with each other while in flight; then also with the filter media and previously deposited particles via collisions, and finally after depositing, they pose obstacles to the fluid flow. The shapes of the particles are not known and the adhesion or stickiness between particles, and between particles and filter media are not known. Additional forces such as electric charges may have to be considered, yet neither the charges on the particles nor those on the filter media are known. When the force exerted by the flow becomes too large, or the direction of the flow is reversed (pulse cleaning), particles that were previously deposited may come loose again and break off in larger chunks. And all of these effects occur on scales from about 50 nanometers to several meters, from the smallest particles to the

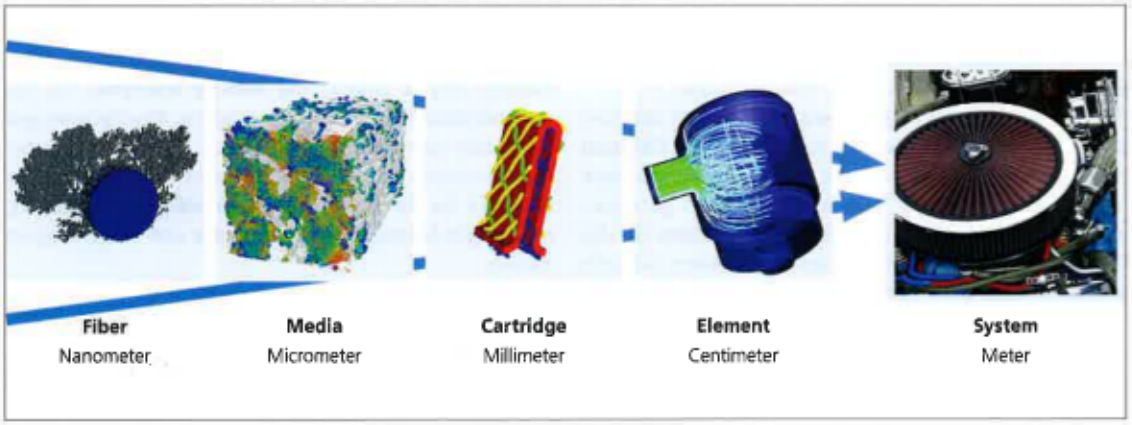

Fig. 1: The Scales of filtration considered in this work cover the filter media and cartridge ranges.

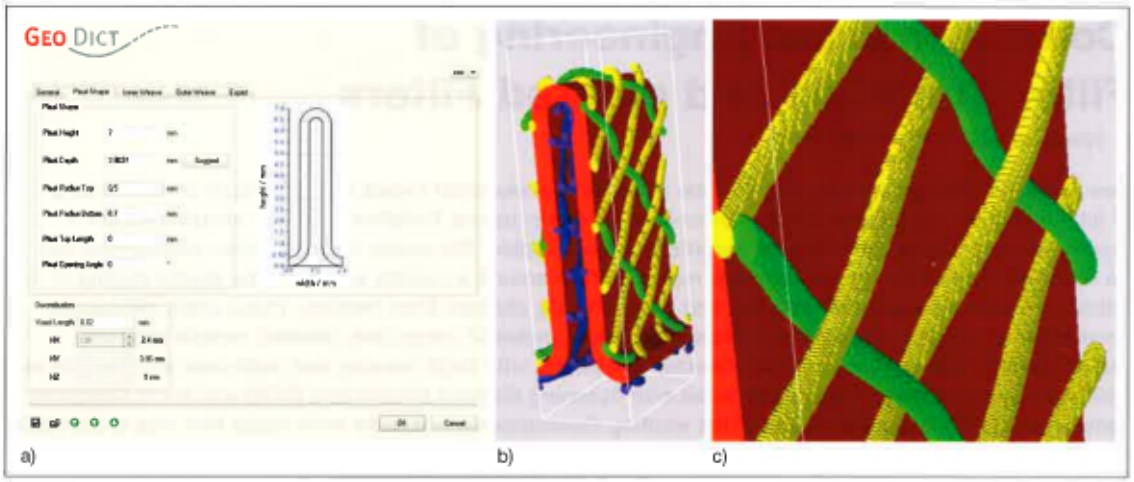

Fig. 2: a) CAD drawing of pleated filter media, b) computational grid image for this pleat including inner and outer support mesh consisting of 120 x 193 x 450 cells and c) detail from b) revealing the cube-shaped individual cells of the computational grid.

length of the exhaust system of a vehicle. So, from a simulation view point, particle filtration simulation poses three different types of difficulties:

1. The process is not completely understood.
2. The process is understood, but its parameters are not known.
3. The process and its parameters are known, but proper modeling would overwhelm the computational resources.

Progress is made with respect to all three of the above. A basic ingredient for this progress is the availability of new hardware. µCT gives unprecedented insights into the three-dimensional structure of filter media. Based on µCT it is possible to create sophisticated computer models of the filter media that ultimately allow the design of the filter media for specific applications. Atomic force microscopy (ATM) is used to determine the adhesion forces between different materials. Such data is essential in the regime where some, but not all, colliding particles get collected. And last but not least, the progress in hardware has made possible detailed three-dimensional computations on affordable computers that were unconceivable just a few years ago.

Besides the progress in hardware, new models and new algorithms also contribute to the progress in filtration simulation. Most notable for the models are the influence of electric fields in air filtration, stochastic geometry models for random filter media, incorporation of slip flow, treatment of particle collisions and bounce, subscale models of filter cake as porous media, and the introduction of the Stokes-Brinkman equations for handling regimes of free and porous media flow that are so dominant in filtration applications. On the simulation side, the parallelization of the flow solvers and the particle tracking codes, task automation, handling and result extraction from massive result data sets, and vastly improved pre- and post-processing capabilities are available today.

2. Filter media and pleat simulation

Detailed numerical simulations are based on realistic three dimensional geometric models [1]. To validate the simulation, existing filter and filter media must be imported into the computer. CAD data sets are commonly available for the filter. For the filter media, usually microscopy, SEM or µCT images are obtainable. The 3D model of the filter or filter media is partitioned into small cells, the computational grid, to perform the simulations. The fundamental approach in our work is to directly use 3D-images as the computational grid of, typically, between 1 million and 100 million cube-shaped cells. The simplification compared to µCT lies in the number of colors. Colors represent different materials and their properties, e.g. pores, polyester, ceramics, warp or weft wires, etc. Hence computational grid images (referred to from now on as structures) often contain only 2 colors, and usually less than 10. All representations, µCT, CAD or analytic descriptions, get ultimately converted into structures. Figure 2 illustrates the conversion from a CAD and mesh description to a structure for the case of an individual pleat consisting of a single-layered media and inner and outer support meshes.

Structure generators create structures of filter media based on analytic or statistical data. Even designs that do not exist in reality can be considered and compared. The fact that structures are simplified images has one further advantage besides the automatic grid generation. Structures can be directly displayed and compared with

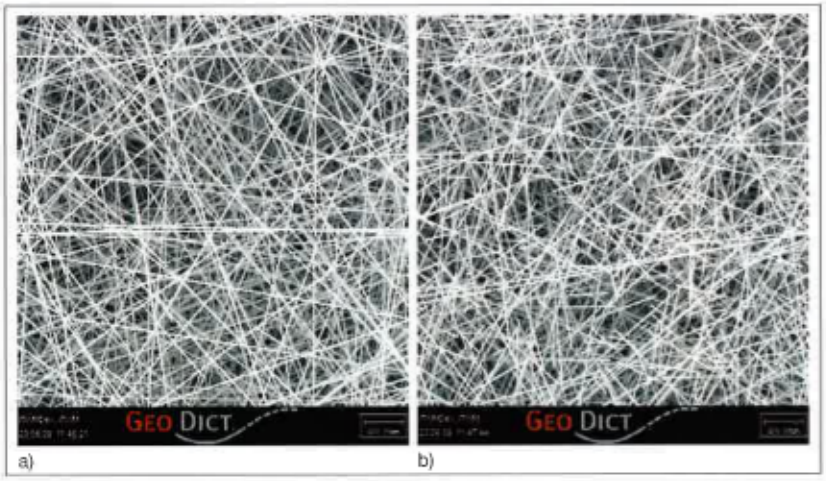

Fig. 3: SEM visualization of 8 volume percent 5 micron fibers at anisotropy 100 (a) and at anisotropy 7 (b), following [5].

images of real objects. We distinguish 2D slice visualization, 21/2 D SEM visualization and 3D visualization. All simulation images are created with the software GeoDict, [7]. We consider two structure generators in exemplary fashion. For a comprehensive overview, see [10].

2.1 Nonwoven filter media.

The nonwoven generator takes few input parameters. They are the porosity of the nonwoven, the fiber diameter and a parameter describing the probabilities of the fiber directions, relating the through-plane to the in-plane component of the fiber directions [5]. In addition, the fiber's cross-sectional shape, fiber length, fiber mix, etc., help to completely characterize many synthetic fibers. The generator works by randomly picking positions and directions for the fibers with appropriately defined probability densities, and then placing the fibers in the initially empty structure that later represents the nonwoven.

Thus, besides the fibers, the size of the initially empty structure must also be selected. For filtration applications, the through-plane direction is completely covered. For the two lateral directions, large enough in-plane cutout lengths must be considered so that the predicted pressure drop, filter efficiency and filter life time are representative. Representativeness is ensured by verifying, that the results do not change much if the simulations are repeated after fiber generator is run again with a different sequence of random numbers drawn from the same distributions.

Figure 3 illustrates the effect of the anisotropy parameter. The value 100 leads to fibers aligned almost perfectly in the plane (a). The smaller anisotropy parameter 7 leads to the orientation shown on the right, where fibers have a clear out-of-plane component. Each structure consists of 1000 x 1000 x 400 cells and requires 200 MB of memory. The generation takes about 10 seconds on a laptop. Here, the resolution was 1 µm so that 5 micron fibers appear as 5 grid cells.

2.2 Woven filter media.

The woven structure generator [3] applies both to textiles and metal wire meshes, and takes as basic input the weave type, aperture and thread thicknesses or wire thicknesses. Mono-filaments and multi-filaments are possible. On top of that, additional options exist regarding the crank, broadening, lateral deformations etc. for the yarn or wires. The woven structure generator starts with an initially empty structure and places threads or wires in selected cells. Woven are in principle deterministic, i.e. threads or wires are always in the same position. However, in real production processes some randomness or tolerances occur – hence, the woven generator relies on a random number generator, for example to place the individual filaments in a multi-filament textile – see Figure 4.

For woven, the size of the structure is determined by the textile parameters. A single copy of the pattern is representative of the woven and creates the lowest computational effort. The second factor determining this effort is the resolution. The smallest cross sectional dimension should be resolved by 5-6 grid cells, so that 10 micron filaments mandate 1.6 micron resolution and the pattern of Figure 4 a) requires about 510 x 510 x 260 grid cells.

2.3 Pleat model for cartridge filters.

When the effects of the pleat shape, height and width must be considered, another scale comes into play. On this scale, the filter media is modeled as homogenized cells with defined permeability. It may be set separately for each layer of a filter media [9]. Another question of

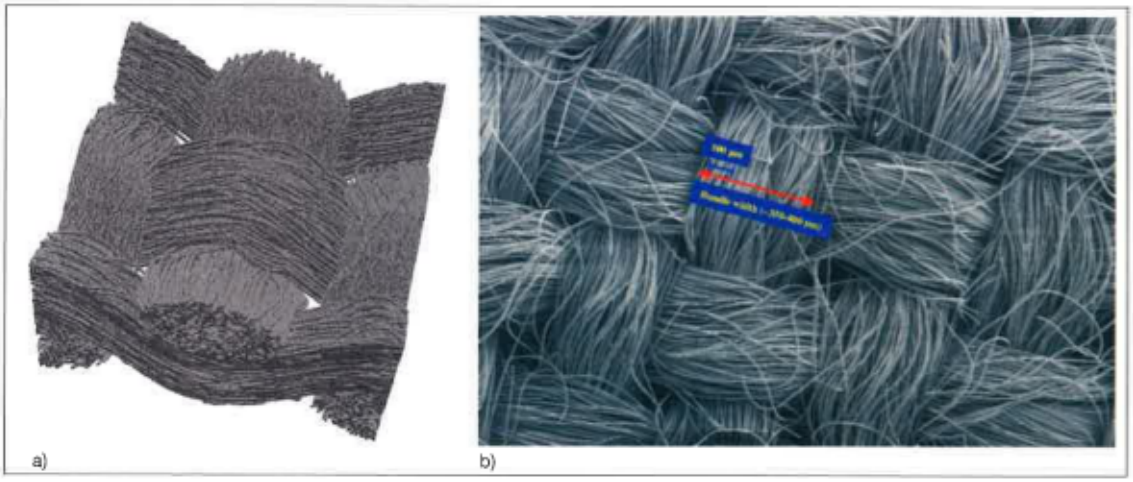

Fig. 4: 3D Visualization of a generated structure (a) and SEM of a carbon fiber multi-filament woven (b, courtesy of Jeff Gostick, University of Waterloo).

wide interest is the influence of support structures on the pressure drop across a pleated filter. Such structures serve to keep the outflow region of the pleat open which is necessary not to invoke an undue increase of the overall pressure drop [8]. The support structures may lower the initial pressure drop by as much as 40% if used appropriately. In the example in Figure 2 b) a woven wire mesh in blue, with cyan warp and weft wires, is used to keep the red filter media apart. The yellow and green wires model a protective outer mesh.

3. Pressure drop simulation

Once the filter media model is accepted, filtration simulation poses increasingly difficult tasks. The challenges range from the geometric characterization of pores [10] through the computation of the pressure drop, all the way to simulating filter efficiency and filter life time [10].

We consider purely viscous, incompressible fluids and stationary flows, so that there is no time-dependence. Conservation of momentum and conservation of mass can be written as stationary Navier-Stokes equations in the pressure – velocity formulation as follows:

$$-\mu\Delta\vec{u}+(\rho\vec{u}\cdot\nabla)\vec{u}+\nabla P=\vec{f}$$

(NS conservation of momentum) (1)

$$\nabla\cdot\vec{u}=0 \text{ (conservation of mass)} \quad (2)$$

In equations (1) and (2) $\vec{u}$ is the fluid velocity is the density, p is the pressure, μ is the fluid viscosity and $\vec{f}$ is a force density. The simulations compute $\vec{u}$ and p for a given pressure drop ΔP by converting ΔP into a force density and using periodic boundary conditions on the computational box (c.f. white edges in Fig. 5). On the surfaces of solid obstacles, the no-slip boundary condition (3) is used:

$$\vec{u}=0 \text{ (no slip boundary condition)} \quad (3)$$

Since in most filtration settings the mass flow is prescribed, ΔP is adapted until the computed mass flow matches the prescribed one.

The flows in most filter media are so slow that due to its negligible influence one may drop the inertia term from the conservation of momentum in the Navier-Stokes equations (1) to reach the Stokes equations.

$$-\mu\Delta\vec{u}+\nabla P=\vec{f} \text{ (Stokes conservation of momentum)} \quad (4)$$

The main benefits of using the linear equations (2), (3) and (4) are that the solvers converge more quickly and that the flow field needs not be recomputed to achieve a prescribed mass flow. For the Stokes equations, simply multiplying velocity field and pressure can be used to match the prescribed mass flow.

When the particles are much smaller than the scale of the filter media, or when the scale of the filter media is much smaller than that of the pleat, a third set of equations comes into play: the Navier-Stokes-Brinkman equations [4]. The additional term accounts for porous media formed by the sub-grid sized particles on the surfaces of the filter media or for the fibrous filter media that cannot be resolved on the scale of a complete pleat. The equations couple the free flow in the pores with the so-called Darcy flow in porous media

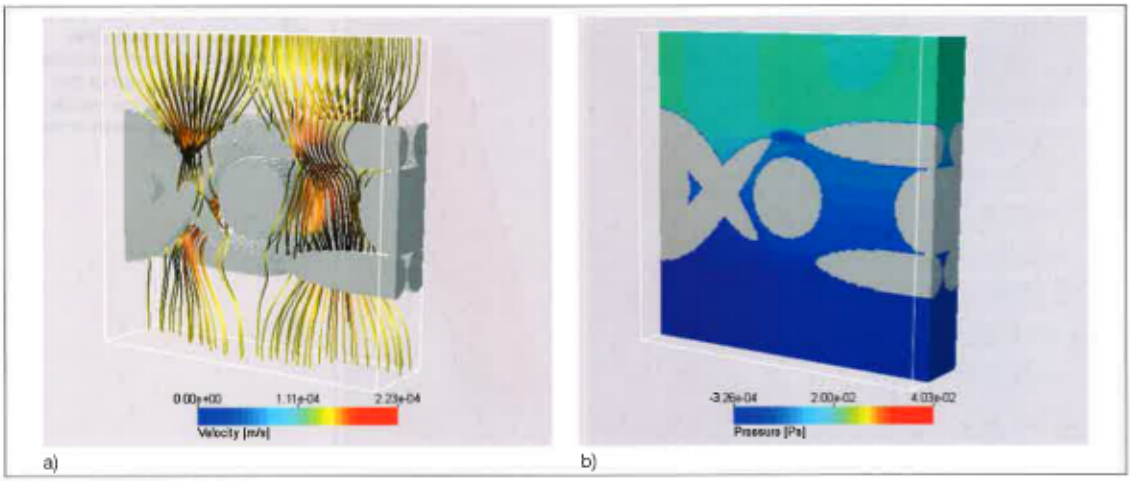

Fig. 5: Stream lines (a) and pressure (b) computed for the flow through a Dutch weave metal wire mesh in a computational box illustrated by its white edges.

$$-\mu\Delta\vec{u}+(\rho\vec{u}\cdot\nabla)\vec{u}+\mu K^{-1}\vec{u}+\nabla p=\vec{f}$$

(NS-Brinkman conservation of mom.) (5)

K^{-1} is the inverse of the permeability tensor and μK^{-1} is the flow resistivity. In the free flow regime in the empty cells, K^{-1} vanishes so that equation (5) becomes equation (3). In the porous cells K^{-1} becomes quite large, and the velocity $\vec{u}$ small. In that regime, the velocity terms on the left of equation (5) may be neglected and we find Darcy's law

$$\vec{u}=-\frac{K}{\mu}(\nabla p-\vec{f})\ \text{(Darcy's law)} \quad (6)$$

By combining the equations for the unconstrained flow and flow in porous media, the pressure drop of cartridge filters (see section 4) can be computed.

For the varying requirements of the Navier-Stokes, Stokes and Stokes-Brinkman equations, several solution methods are available. The ParPac Lattice-Boltzmann code [2] for all three sets of equations is very well parallelized and works on very large structures on distributed memory machines. A finite volume code SuFiS® (see [4]) also for all three sets of equations is designed for computations of complete filters, including the housing. Another class of finite volume codes, FFF-Stokes [6] solves only Stokes flow. However, it has the lowest memory requirements and shortest solution times for highly porous media.

There are several challenges for the computation of flow fields for resolved filtration simulations. The first is the need for an accurate geometric representation of the filter media and its translation into a computational grid. This challenge is met for a variety of structures, as seen in section 2. The structure is simply identical with the computational grid, different from other approaches followed for example by Fluent®, CFX® and Star-CD®. Because the computational domains become very large, highly efficient codes in terms of memory and run-time are necessary. The regular behavior of the structure helps saving memory for coordinates, sophisticated new algorithms are used and the power of modern computers is utilized by parallel implementations. While the current state of the art for structures with about 1,000 x 1,000 x 1,000 cells is sufficient for the prediction of the pressure drop and deposition of large particles, nano particles and nano fibers require even better resolved obstacle surfaces [10].

4. Simulation-based design of a new hydraulic filter element

A highly improved next generation filter element was developed based on pleat geometry and flow simulations with experimental validation. The new filter element exhibits a significantly lower pressure drop while achieving the same filter efficiency and same filter capacity as the previous generation.

Very high oil pressures are intrinsic to mobile hydraulic applications. Under such high pressures, the individual pleats of a pleated filter tend to collapse and thus, significantly diminish the accessible filter media surface. In order to prevent such collapse, supporting meshes can be used both on the outside and inside of the filter media. Computer simulations predicted that a new design, in which the weave type in the outflow channel

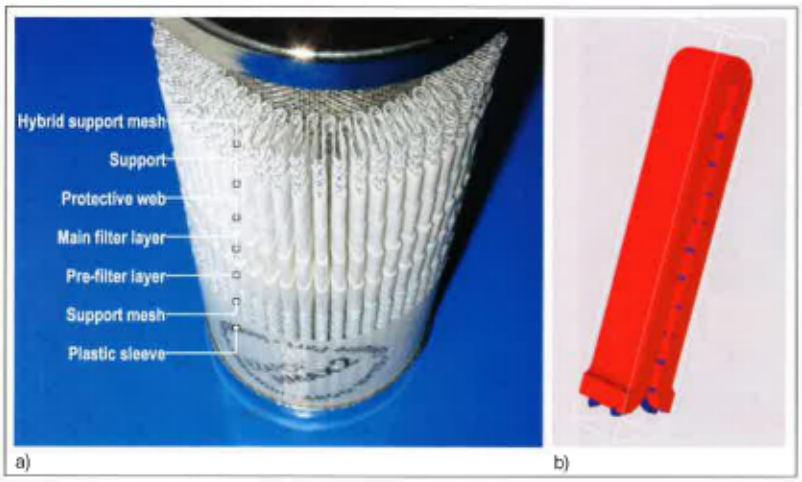

Fig. 5: Detail of the new hydraulic filter element with twill inner support mesh (a) and computer model of a single pleat of this filter element with filter media in red and supporting mesh in the outflow channel (b).

of the pleat is changed from plain weave to 2/2 twill, would lower the pressure drop of the filter element by 30 % while maintaining the good performance with respect to filter efficiency and filter capacity. One main benefit of the computer simulations was the establishment of this improvement. Very few prototypes needed to be built, and they simply verified these predictions. The second benefit was that the simulations identified a set of optimal yet stable parameters. Thus, small variations in the production process do not disturb the performance of the filter element.

To establish the validity of the methodology, the existing filter element including the plain weave support structure was modeled. Figure 5 a) shows a cut up filter element that shows the filter media with the new twill inner support mesh. For simplicity the multi-layered filter media was modeled as a single layer, shown in red in Fig. 5 b).

Comparison with measurements for the existing plain weave filter element allowed the determination of a few model parameters, such as the indentation of the wires into the filter media. Then, these parameters were preserved while design parameters, such as wire diameters and weave pattern, were varied. The geometric models confirmed what had been suspected by the designer: for the plain weave, there exist settings where the blue

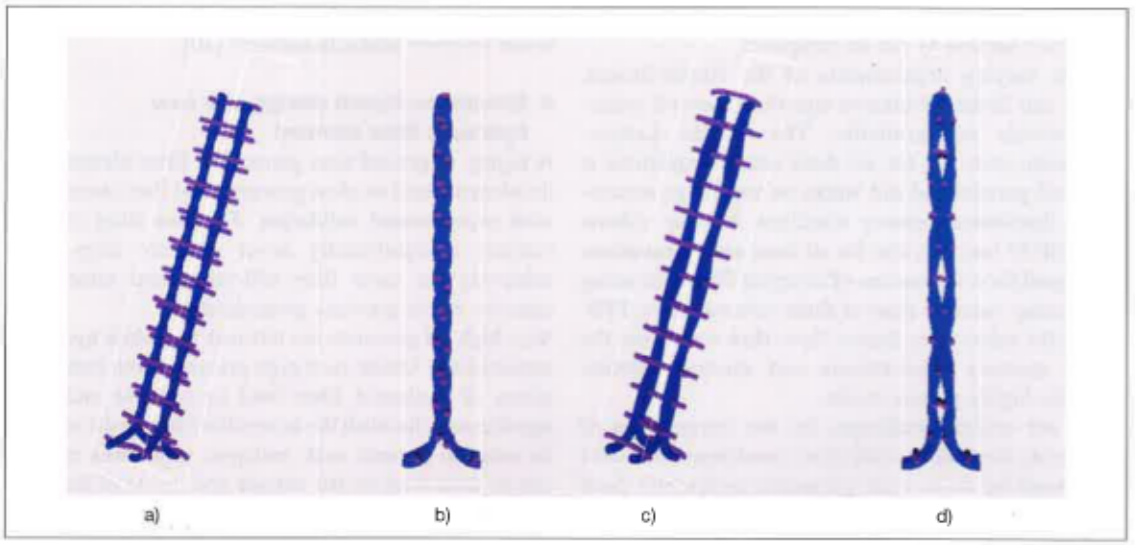

Fig. 6: The main difference between the original and the new design. The plain weave a), b) allows the blue wires to slide next to each other and creates a rather narrow outflow channel. For the same wire thicknesses, the 2/2 twill c), d) prevents the wires from sliding next to each other and creates a wider outflow channel.

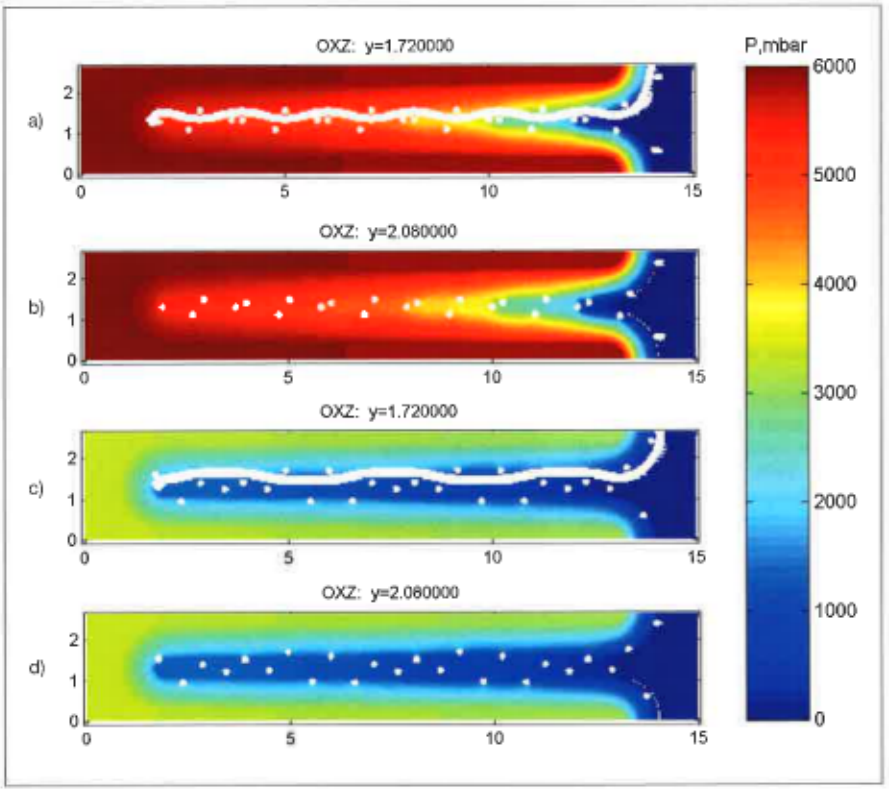

Fig. 7: a), b) show the pressure distribution ($p+\int f$ in the notation from equation (5)) for the plain weave for two different cross sections. c), d) show the pressure distribution for the 2/2 twill for the same areas. White areas mark the solid wires. The filter media is not shown but it can be envisioned from the strong gradients in the pressure fields.

wires in figure 6 can lie in a plain (figure 6 b)). For the 2/2 twill this configuration cannot occur (figure 6 d)). The impact on the pressure drop is tremendous. Figure 7 a), b) show the pressure distribution for flow from left to right for the plain weave for two different cross sections while c), d) show the pressure distribution for the same mass flow and same wire diameters for the 2/2 twill. For the twill, a 35% decrease in the overall pressure drop occurs. The simulation results clearly illustrate the reason for this phenomenon. For the plain weave, there is a significant gradient in the pressure along the outflow channel, from left to right in figure 7 a), b). For the twill, the outflow channel shows pressure values very close to that of the outlet all through.

With this strong evidence from the simulations, making a prototype became worthy. For the configuration as shown, the same 35% pressure drop reduction as predicted by the simulations was found to occur in reality. For some other design with longer pleats, up to 45% improvement in the pressure drop could be achieved. Additional measurements showed that the filter efficiency and filter life time are not affected by the change in support mesh. The improvement is hence so significant that the design was patented [11] and is now on the market as Argo-Hytos' EXAPOR®MAX 2 hydraulic filter element.

5. Conclusions and outlook

We have demonstrated that computational experiments provide a way of rapid prototyping filtration applications and can provide invaluable detailed insights into filtration processes that help designing better filters for applications essential to the world's ecological balance. The project described in section 4 led to a patent by Argo-Hytos on their new hydraulic filter element EXAPOR®MAX 2 . The pressure drop of EXAPOR® MAX 2 is between 30% and 45% lower than that of the previous filter element generation. The work in section 4 also laid the foundations for new computer software. The modules PleatGeo and PleatDict for ITWM's GeoDict Software [7] are tailor-made and easy-to-use for the simulation and design of pleated filters. Other GeoDict modules exist that model various filter media and can compute the pressure drop, filter efficiency and filter life time for such filter media.

Literature

[1] A. Latz and A. Wiegmann, Simulation of fluid particle separation in realistic three dimensional fiber structures, Filtech, vol. I, 2003, pp 353-361.

[2] I. Ginzburg, P. Klein, C. Lojewski, D. Reinel-Bitzer, K. Steiner: Parallele Partikelcodes für industrielle Anwendungen, Verbundprojekt im Rahmen des HPSC, Abschlussbericht, Fraunhofer Institut für Techno- und Wirtschaftsmathematik (ITWM) Kaiserslautern, März 2001.

[3] E. Glatt, S. Rief, A. Wiegmann, M. Knefel and E. Wegenke, Struktur und Druckverlust realer and virtueller Drahtgewebe, Filtrieren und Separieren, Vol. 23, No. 2, 2009, pp 61-65.

[4] O. Iliev, V. Laptev: On Numerical Simulation of Flow through Oil Filters, J. Computers and Visualization in Science, vol. 6, 2004.139-146.

[5] K. Schladitz, S. Peters, D. Reinel-Bitzer, A. Wiegmann, J. Ohser, Design of acoustic trim based on geometric modeling and flow simulation for nonwoven, Computational Material Science, Vol. 38. No 1, 2006, pp 56-66.

[6] A. Wiegmann, Computation of the permeability of porous materials from their microstructure by FFF-Stokes, Berichte des Fraunhofer ITWM, Nr. 129, 2007.

[7] A. Wiegmann, GeoDict, Fraunhofer Institut für Techno- und Wirtschafts-mathematik, http://www.geodict.com, 2010.

[8] A. Wiegmann, L. Cheng, E. Glatt, O. Iliev and S. Rief, Design of pleated filters by computer simulations. Annual Meeting of the American Filtration and Separation Society, Minneapolis, MN, USA, 2009.

[9] A. Wiegmann, S. Rief and D. Kehrwald, Computational Study of Pressure Drop Dependence on Pleat Shape and Filter Media, Filtech, Vol. I, 2007, pp 79-86.

[10] A. Wiegmann, S. Rief, A. Latz and O. Iliev, Toward Predicting Filtration and Separation: Progress & Challenges, Filtech, Wiesbaden, Deutschland, Vol. I, 2009, pp 48-63.

[11] A. Schindelin and W. Schadt, Corrugated or folded flat material. International Patent Publication number WO/2009/026978.

Andreas Wiegmann, Oleg Iliev
Fraunhofer ITWM
Fraunhofer-Platz 1
67663 Kaiserslautern
Andreas Schindelin
ARGO-HYTOS GMBH
Industriestraße 9
76703 Kraichtal-Menzingen